Available online at www.dergipark.org.tr/en

INTERNATIONAL ADVANCED RESEARCHES and ENGINEERING JOURNAL

Journal homepage: www.dergipark.org.tr/en/pub/iarej

e-ISSN: 2618-575X

International Open Access

Volume 05
Issue 03

December, 2021

Research Article

Harmonic response analysis of elliptically curved thin plates

Oğuzhan Daş [a]

[a]*Dokuz Eylul University, Department of Motor Vehicles and Transportation Technologies, Izmir, 35700, Turkey*

ARTICLE INFO

Article history:
Received 27 July 2021
Revised 19 September 2021
Accepted 07 October 2021

Keywords:
Elliptically curved plates
Finite element analysis
Harmonic response

ABSTRACT

In this study, harmonic response analysis of isotropic elliptically curved thin plate structures has been conducted. The structure has been excited by a harmonic load, whose maximum magnitude is 100 N. The structure has been considered under fixed from both straight edges boundary conditions. The effect of the elliptical geometry on the harmonic response of the structure in terms of the critical frequency region, phase angle, stress, and displacement has been examined. For this purpose, the vertex to co-vertex ratio has been variated from 3 to 4 by 0.1 intervals. All analyses have been performed via ANSYS Workbench by employing the Mode Superposition Method. The results indicated that the elliptical geometry has a significant impact on the harmonic response of elliptically curved thin plate structures.

1. Introduction

The vibration behavior of a structure is a significant research field in which researchers conducted various studies to understand the effects of damage [1-3], geometry [4-6], material [7-9], and other parameters [10-17] on this concept. Related to vibrational behavior, the harmonic response is another essential concept for understanding a steady-state response of a structure under sinusoidal loads. The principal interest of the harmonic response analysis is the resonance frequency region since excessive vibrations, stress, displacement, and noise occurs near or at that region. Some studies that cover vibration analysis including the harmonic response of various structures have been briefly presented as follows. Kıral examined the harmonic response of laminated composite beams under various boundary conditions and considering different stacking sequences [18]. Ramesha et al. performed a modal analysis and harmonic response analysis of free-free and ball bearing constrained crankshaft considering 0 -5000 Hz excitation frequency range [19]. Yu et al. conducted both modal and harmonic response analysis of some key components of a ditch device [20]. Zhang et al. employed a harmonic analysis for coupled plate structures by considering the dynamic stiffness method [21]. Jiaqiang et al. measured the harmonic response of a solar dish power generation system considering the wind-induced vibration [22]. Çeçen and Aktaş performed both modal and harmonic response analyses of carbon fiber laminate reinforced concrete railway sleepers [23]. Rahmani and Moslemi Petrudi examined the nonlinear vibrations and dynamic response of self-excitation of a cantilever nanocomposite tube, which contains flowing fluid. They employed Galerkin Method and Euler-Bernoulli Beam Theory to solve the corresponding Ordinary Differential Equations to evaluate the behavior of the structure [24]. Cruceanu and Sorohan employed the Finite Element Analysis to evaluate the harmonic response of a railway wheelset [25]. Zeng et al. investigated the vibration response characteristics of a cracked rotating compressor blade using the Finite Element Analysis. They measured the impact of the aerodynamic force, angular acceleration, and crack properties on the vibrational characteristics of the compressor blade [26]. Jena et al. performed a dynamic response analysis for fractionally damped beam structures under external loads. They employed Homotopy Analysis Method to evaluate the vibrational response of the beam structure [27]. Gawryluk et al. measured the dynamic response of a composite beam, which rotates at a constant speed due to harmonic excitation. For this purpose, they used the Finite Element Method and an experimental setup [28]. Son et al. performed a shock and harmonic response

* Corresponding author. Tel.: +90-232-632-1248 (139).
E-mail addresses: oguzhan.das@deu.edu.tr *(O. Daş)*
ORCID: 0000-0001-7623-9278 *(O. Daş)*
DOI: 10.35860/iarej.975247

analysis for unmanned aerial vehicle's nose landing gear having air damper. They built a dynamic model which comprises a main mass and a wheel mass that are linked to each other by U-shaped landing gear. They evaluated the harmonic response of the system by considering the ratio between the displacement amplitude and the amplitude of the base excitation [29]. Kumar and Sarangi used the Finite Element Method to conduct the harmonic response analysis for carbon nanotube-reinforced functionally graded beam structure. For this purpose, they considered X, Δ, and O type functionally graded carbon nanotube beam structures modelled in ANSYS [30]. Praharaj and Datta investigated the dynamic behavior of thin plate structures subjected to a moving load and resting on a fractional viscoelastic foundation. They examined the effects of the foundation parameters, fractional-order derivative, acceleration, and velocity of the subjected moving load on the dynamic response of the structure [31]. Abed and Majeed measured the impact of the boundary conditions on the harmonic response of cross-ply and angle-ply composites having different materials and thicknesses [32]. Aghazadeh investigated the dynamics of fluid conveying axially functionally graded pipes. For this purpose, a higher-order shear deformation theory is employed to satisfy zero-shear conditions to obtain realistic results [33]. Liu et al. examined the dynamic response of curvilinearly stiffened plates by employing the Finite Element Method. They measured the influence of the temperature on the dynamic behavior of the isotropic structure [34]. Alavi and Eipakchi evaluated the dynamic response of viscoelastic annular sector plates subjected to asymmetric impulsive and harmonic transverse force. They used Hamilton's principle to derive the equation of the motion by considering the first-order shear deformation theory [35]. Heydarpour et al. developed a differential quadrature method based on the Heaviside function and a non-uniform rational B-spline-based multi-time integration scheme to examine the nonlinear dynamic response of laminated composite cylindrical shells. They measured the impacts of the geometrical properties, impulse loading types, time durations, loading location, and the number of layers on the nonlinear dynamic response of the structure [36]. Yulin et al. investigated the dynamic response of a three-beam system having intermediate elastic connections, under mass-spring, and subjected to a moving load. For this purpose, they employed the Finite Sine-Fourier Transform to obtain the dynamic ordinary differential equations, which are solved to evaluate the dynamic response of the structure [37]. Eyvazian et al. investigated the dynamics of nanocomposite cylindrical shells subjected to a moving harmonic load. For this purpose, they employed the first-order shear deformation theory in accordance with the nonlocal strain gradient theory to obtain the equations of motion of the cylindrical nanoshell resting on an elastic foundation [38]. Oke and Khulief performed a dynamic response analysis for fluid conveying composite pipes whose inner wall has a surface discontinuity. For this purpose, they employed Hamilton's principle and wavelet-based Finite Element Method [39].

Elliptically curved plate structures are employed in various engineering fields such as aerospace, automotive, ships, etc. Therefore, investigating the harmonic response of elliptical plates considering their geometry can provide significant knowledge to these fields. To the best of the author's knowledge, although numerous studies address the harmonic response of various structures, the harmonic response of elliptically curved structures has not been covered. Besides, the effect of the structure's geometry on the harmonic response has not been measured in the literature.

In this study, the harmonic response of the isotropic elliptically curved thin plates has been investigated. Besides, the effect of the structure's geometry on the harmonic response has been examined by variating the co-vertex – vertex ratio. For these purposes, the structures have been modeled via the commercial finite element software ANSYS [40]. The co-vertex – vertex ratio values have been ranged from 3 to 4 by 0.1 intervals. The harmonic response analyses have been conducted by considering a sinusoidal load, which alternates between 0-100N. The damping ratio has been chosen as ξ=0.02 [18]. The analysis results have been interpreted by considering the variation of the resonance frequency, maximum stress, and deformation at the resonance frequency. The contributions of the study can be expressed as follows:

- Investigating the free vibration and harmonic response characteristics of an elliptically curved thin plate structure.
- Examining the effect of the structural dimensions on the first two natural frequencies of the elliptically curved thin plate structure.
- Measuring the impact of the co-vertex – vertex ratio of the elliptically curved plate on the phase angle and critical frequency value where excessive vibrations occur.
- Measuring the impact of the co-vertex – vertex ratio of the elliptically curved plate on the maximum response and maximum stress occurred due to the subjected harmonic load.

2. Harmonic Response Analysis

The harmonic response analysis has been evaluated considering the governing equation of motion of the system, which is

$$M\{\ddot{q}\} + \dot{C}\{\dot{q}\} + K\{q\} = \{F\} \quad (1)$$

where M, C, and K are the mass, damping, and stiffness

matrix respectively. $\{q\}$ represents the generalized displacement vector including in-plane and out-of-plane displacements [41] and F is the harmonic (sinusoidal) force which can be written in complex notation as:

$$F = F_{max} e^{j\alpha} e^{j\omega t} \quad (2)$$

where ω and α is the excitation frequency and the phase angle of the applied force, respectively. The response of a system is also harmonic, which can be defined as:

$$y = y_{max} e^{j\eta} e^{j\omega t} \quad (3)$$

where η is the phase angle of the response. It can be concluded from the Equations (2) and (3) the phase angles of the load and response can be different, while the frequencies should be the same. Note that the phase shift of the force may exist if multiple loads are applied in different phase angles. Besides, the displacement phase shift may be present in the existence of damping or applied forces. [42] The mass, damping, and stiffness matrices can be evaluated by employing the Classical Plate Theory. The corresponding mathematical expressions and considered assumptions can be found in any textbook [41].

The solution of the governing equation given in Equation 1 in the presence of harmonic loads is:

$$(-\omega^2 M + j\omega C + K)\{y\} = \{F\} \quad (4)$$

Following the brief harmonic response theory given above, the harmonic response analysis of elliptically curved thin plates has been conducted via ANSYS Workbench 18.2 software. For this purpose, a number of 1000 SHELL181 elements have been considered since the SHELL181 element satisfies the assumptions and required degrees of freedom for a thin structure [41]. As seen from Figure 1, the structure has fixed from both straight edges. A distributed harmonic force with 100 N maximum magnitude and 0^0 phase angle has been applied. To measure the effects of the structural geometry on the harmonic response, the ratio of the vertex-co-vertex (R_c) has been increased from 3 to 4 by considering 0.1 intervals. The thickness of the structure is remained constant everywhere and is taken as 1.5 mm. As seen from Figure 2, other geometrical parameters have been considered as independent and constant values. Table 1 presents the considered material properties [41] of the structure to perform harmonic analysis. Before proceeding with the harmonic response analysis, the first two natural frequency values of all structures have been evaluated by performing a free vibration analysis. The results have been evaluated by considering the 0-1500 Hz frequency range to include the second natural frequency values (see Table 2) of all considered structures.

As the solution method, the Mode Superposition Method has been considered since it uses the eigenvectors of the free vibration problem providing accurate results and costs less time when compared with the Full Method [41].

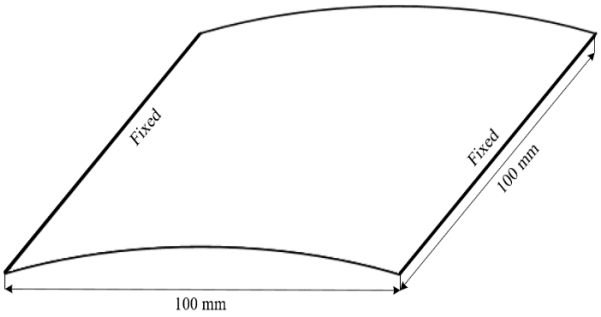

Figure 1. Elliptically curved thin plate

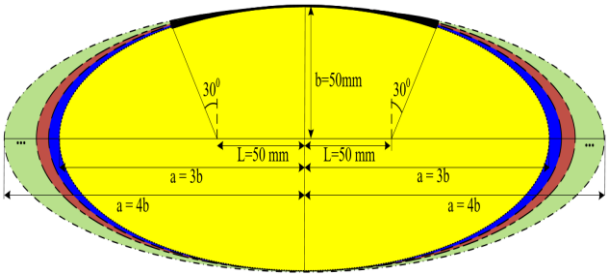

Figure 2. Dimensions of the elliptically curved plate structure

Table 1. Material properties of the elliptically curved thin plate

Property	Symbol	Value
Modulus of Elasticity *(GPa)*	E	200
Shear Modulus *(GPa)*	G	76.9
Density *(kg/m³)*	ρ	7850
Poisson's Ratio	υ	0.3

Afterward, the frequency response and the corresponding phase angle responses have been evaluated for each structure to determine the most critical frequency and corresponding phase angle values for the structure. By using these critical values, the maximum stress and displacement have been obtained. The evaluated results have been interpreted with respect to the change in the R_c.

3. Numerical Results

Table 2 gives the variation of the first two natural frequencies of the elliptically curved structure with respect to changes in respect to the ratio of the vertex to co-vertex (R_c) of the structure.

It is seen from Table 2 that the first two natural frequencies decrease as the R_c value increases. Besides the numerical difference between the first and the second natural frequencies becomes smaller for higher R_c values. Such differences take place due to the difference in the stiffness characteristics of the elliptically curved structure.

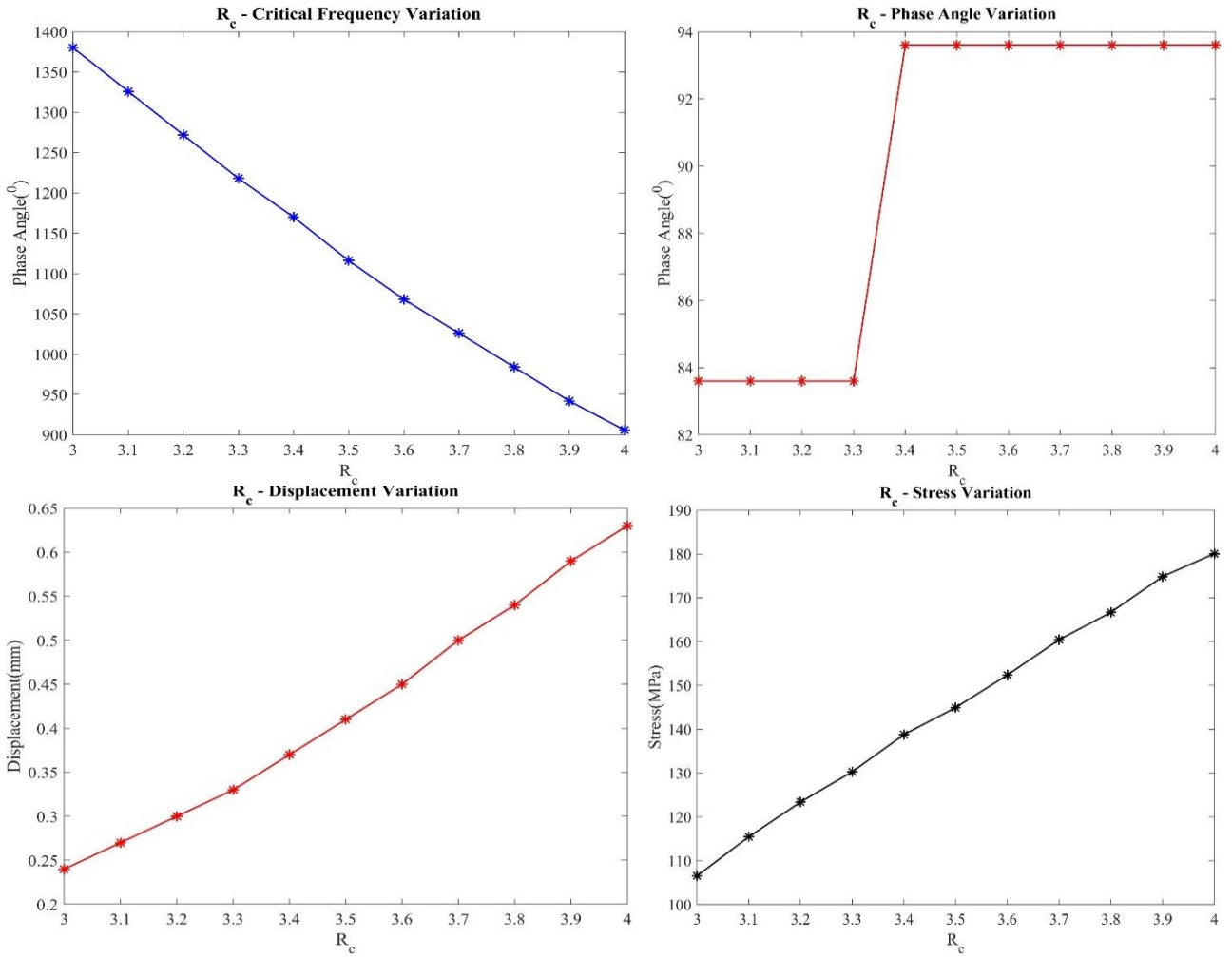

Figure 3. Variation of the fundamental frequency, phase angle, stress, and displacement with respect to R_c

Table 2. The variation of the first two natural frequencies of elliptically curved thin plate structures with respect to R_c

R_c	*3.0*	*3.1*	*3.2*	*3.3*
Freq.1 (Hz)	977.35	973.02	968.97	965.19
Freq.2 (Hz)	1380.90	1328.20	1274.70	1221.50
R_c	*3.4*	*3.5*	*3.6*	*3.7*
Freq.1 (Hz)	961.67	958.39	955.06	952.21
Freq.2 (Hz)	1169.40	1119.10	1070.90	1025.20
R_c	*3.8*	*3.9*	*4.0*	
Freq.1 (Hz)	949.54	941.61	903.63	
Freq.2(Hz)	982.12	947.04	977.31	

Figure 3 gives the variation of the critical frequency, phase angle, stress, and displacement responses of elliptically curved thin plate structure with respect to R_c values. It is seen from Figure 3 that the critical frequency of the elliptically curved structure decreases as the R_c value increases. Besides, the critical frequency has been evaluated close to the second natural frequency for R_c values ranged between 3-3.8. However, it approximates the fundamental frequency for R_c=3.9 and 4.

As seen from Figure 3 that the difference in the critical frequency is almost linear. Since the damping ratio has been considered as ξ=0.02, a difference in phase angle has occurred. The phase angle has been evaluated as 83.6^0 for 3-3.3 R_c values, while it has been obtained as 93.6 for the remained R_c values. In other words, the maximum response occurred at the critical frequency value takes place slightly earlier than the fundamental or the second frequency for R_c values lower than and equal to 3.3 when compared with those frequencies for R_c values bigger than 3.3.

It can be interpreted that the phase angle is not affected considerably by the co-vertex – vertex ratio since the difference is small.

Figures 4 and 5 show the bode diagram of the displacement-frequency response and the phase difference between the response and the applied force for R_c= 3 and 4 respectively. It is seen that the critical response for the structure with R_c =3 has been obtained for the frequency region close to the second natural frequency. On the other hand, the region becomes closer to the fundamental frequency for the structure having R_c =4 ratio. As also seen in Figure 3, the phase angle of the structure having R_c =3 ratio is smaller than those of the structure with R_c =4.

The maximum stress and displacement values have been evaluated for the excitation frequency equal to the fundamental frequency.

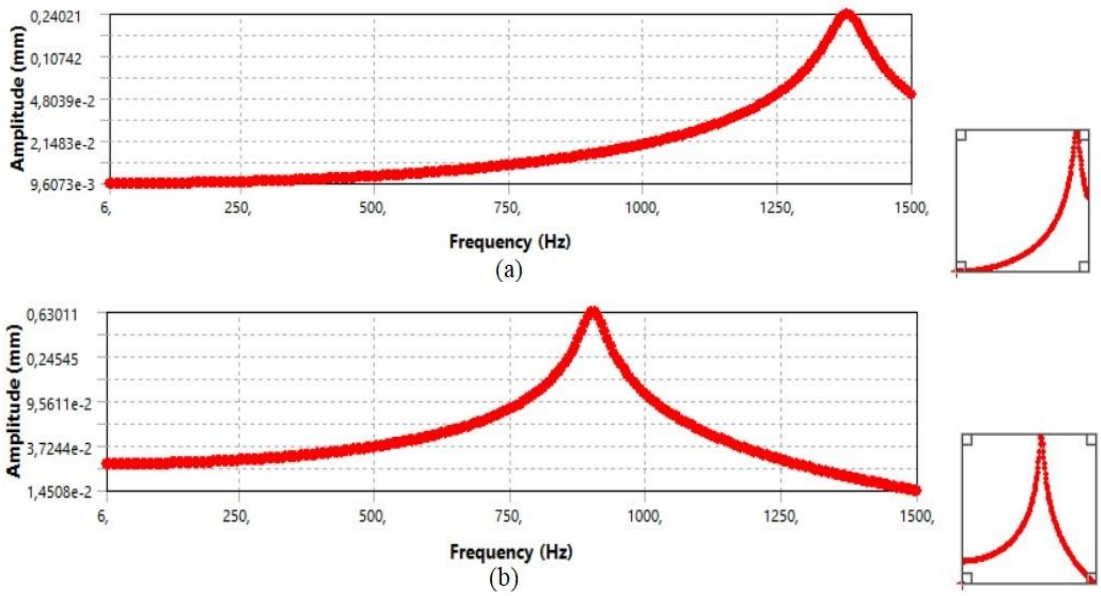

Figure 4. The displacement-frequency bode diagram of the elliptically curved thin plate having (a) R_c=3 and (b) R_c=4 ratio

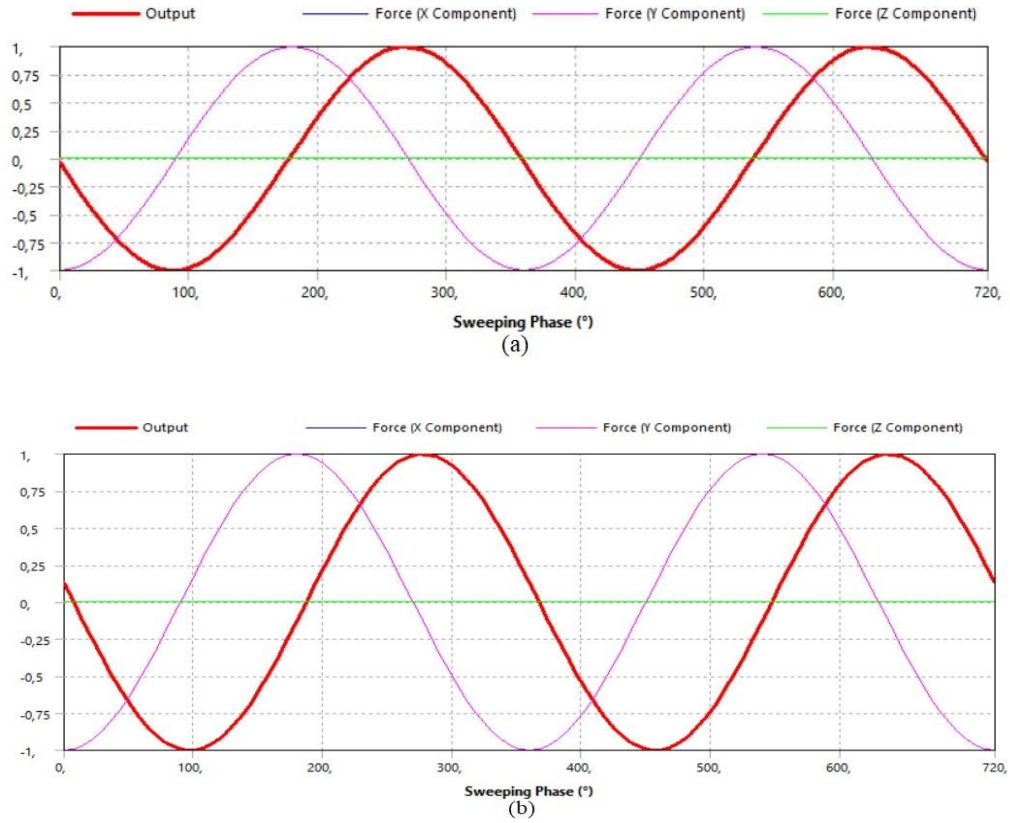

Figure 5. The phase shift between the response and applied force of the elliptically curved thin plate having (a) R_c=3 and (b) R_c=4 ratio

The damping ratio has been taken as ξ=0.02 [18] to prevent the structure from resonance in which failure may occur due to excessive displacement response. As seen in Figure 3, the maximum stress increases as the R_c increases. Similarly, the maximum displacement increases up to 2.5 times as the R_c value reaches 4 from 3. Both displacement and stress values vary almost in a linear form in accordance with the co-vertex – vertex ratio. The maximum stress value is obtained for R_c=4 as 180.07 MPa while the minimum stress is obtained for R_c=3 106.54 MPa. The maximum displacement value is observed for R_c=4 as 0.64 mm whereas the minimum displacement is evaluated for R_c=3 as 0.24 mm.

As seen in Figures 6 and 7, the maximum displacement and stress locations are the same for both R_c=3 and 4. On the other hand, the displacement and stress distributions

vary. It is seen from Figures 6 and 7 that at the most critical frequency, a wider area has been stressed and displaced for the structure with R_c =4 ratio when compared with that of having R_c =3 ratio. The behavior of the structure shown in Figure 6 also represents the second mode shape for R_c=3 and the first mode shape for R_c=4. Therefore, it can be concluded that the maximum stress and displacement occurred in the region where the highest displacements have been observed in the relevant mode shape.

Considering the stress and displacement regions shown in Figures 6 and 7, it is seen that both displacement and stress values in locations close to the fixed edge differ for structures with R_c=3 and R_c =4. It is seen that these values are higher for the structure having R_c=3 than that of R_c=4. A similar interpretation can be made for the width of the displacement and stress regions. As seen from Figures 6 and 7 the displacement and stress regions of the structure having R_c=3 ratio are narrower than these of the structure having R_c=4 ratio regardless of the magnitude of the stress and displacement. Therefore, it can be concluded that the difference in co-vertex – vertex ratio does not only affect the maximum stress and displacement values, but also the distribution of the stress and displacement along with the structure.

4. Conclusions

In this study, harmonic response analysis of elliptically curved thin plate structure has been conducted. The effect of the vertex to co-vertex ratio on the harmonic response has been examined considering the critical frequency region, phase angle, stress, and displacement. All analyses have been conducted by considering the Mode Superposition Method. According to the results of the study, the following conclusions can be drawn.

- The first two natural frequencies of elliptically curved thin plate structures decrease as the vertex to the co-vertex ratio (R_c) increases. Besides, the numerical difference between those two frequencies become smaller as the R_c value increases.

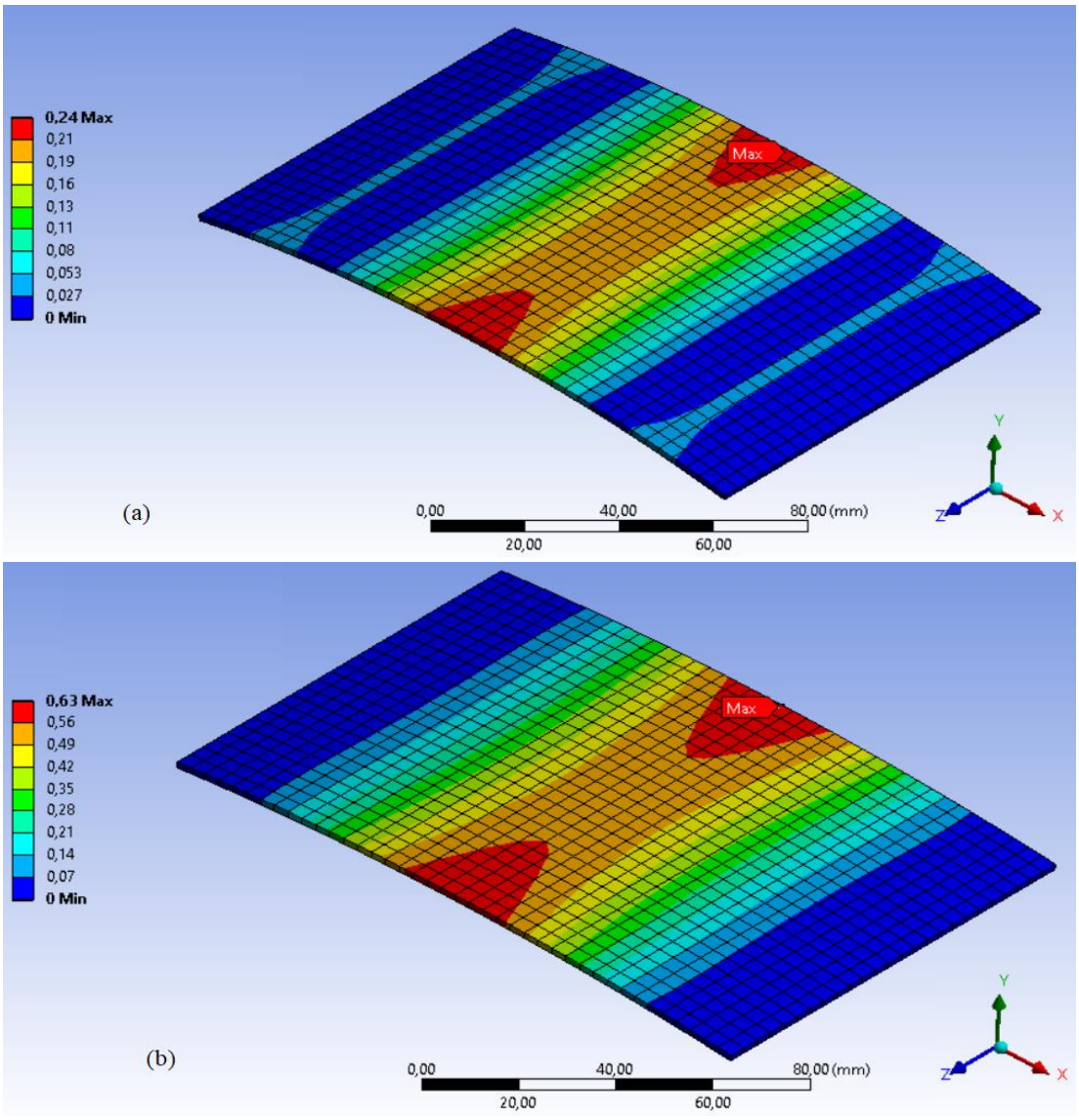

Figure 6. Critical displacement response of the elliptically curved thin plate having (a) R_c=3 and (b) R_c=4 ratio

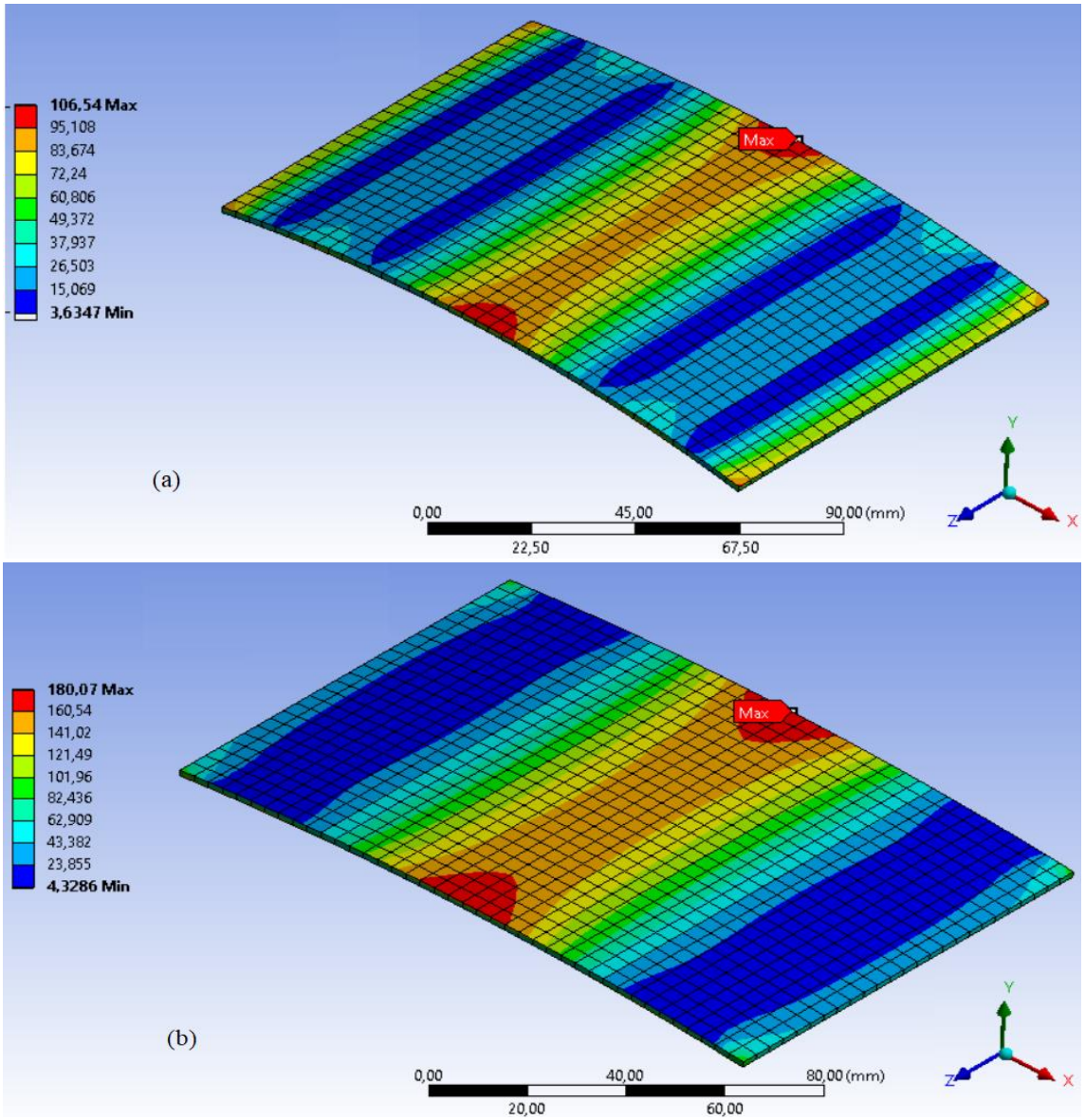

Figure 7. Critical stress distribution of the elliptically curved thin plate having (a) R_c=3 and (b) R_c=4 ratio

- The critical frequency, which causes the highest stress and displacement values, decreases as the R_c ratio increases. Besides, the critical frequency region approximates the second natural frequency for R_c=3-3.8 values whereas it approaches the fundamental frequency for R_c=3.9 and 4.0.
- The phase angle increases from 83.6 to 93.6 for R_c values higher than 3.3
- The maximum stress increases with respect to the increment in R_c values. Likewise, the maximum displacement increases up to 2.5 times as the R_c value increases from 3 to 4.
- The maximum stress and displacement are located in the region where the highest displacement of the relevant mode shapes has been observed.
- The numerical results indicate that the variation of the maximum stress, maximum displacement, and the natural frequency values are almost in a linear form in accordance with the co-vertex – vertex ratio. On the other hand, although it seems that the phase angle changes abruptly as the co-vertex – vertex ratio reaches 3.4, the difference is considerably small. Therefore, it can be concluded that the phase angle is not affected significantly by the change in the co-vertex – vertex ratio.
- It is concluded that the co-vertex – vertex ratio also affects the stress and displacement regions of the structure. The stress and displacement values that occurred near the fixed edges are evaluated higher for the structure having R_c=3 than that of R_c=4. Besides, the stress and displacement regions of the structure having R_c=3 ratio are narrower than those of the structure having R_c=4 ratio regardless of both displacement and stress values.
- The future works may comprise the impacts of the characteristics of the curvature and dimensions of the

structure on the harmonic response of curved structures. Besides, the effects of the fiber orientation on the response of the structure may be examined by taking the plate structure as a composite one.

Declaration

The author declared no potential conflicts of interest with respect to the research, authorship, and/or publication of this article. The author also declared that this article is original, was prepared in accordance with international publication and research ethics, and ethical committee permission or any special permission is not required.

Author Contributions

Oğuzhan Daş: Conceptualization and management of the study, data collection and analysis, interpretation of results, writing the draft and final version of the manuscript.

References

1. Minh, P.P., Do, T. V., Duc, D. H., and Duc, D. N, *The stability of cracked rectangular plate with variable thickness using phase field method*. Thin-Walled Structures, 2018. **129**: p. 157-165.
2. Gonenli, C., and Das, O., *Effect of crack location on buckling and dynamic stability in plate frame structures*. Journal of the Brazilian Society of Mechanical Sciences and Engineering, 2021. **43**: 311.
3. Marjanović, M., and Vuskanović, D., *Layerwise solution of free vibrations and buckling of laminated and sanwich plates with embedded delaminations*. Composite Structures, 2014. **108**: p.9-20.
4. Javed, S., Viswanathan, K. K., Nurul Izyan, M. D., Aziz, Z. A., and Lee, J. H., *Free vibration of cross-ply laminated plates based on higher-order shear deformation theory*. Steel and Composite Structures, 2018. **26**(4): p.473-484.
5. Das, O., Ozturk, H., and Gonenli, C., *Finite element vibration analysis of laminated composite parabolic thick plate frames*. Steel and Composite Structures, 2020. **35**(1): p.43-59.
6. Hongwei, G., Hong, Z., and Xiaoying, Z., *Numerical manifold method for vibration analysis of Kirchhoff's plates of arbitrary geometry*. Applied Mathematical Modelling, 2019. **66**: p.695-727.
7. Belarbi, M., Tati, A., Ounis, H., and Khechai, A., *On the free vibration analysis of laminated composite and sandwich plates: A layerwise finite element formulation.* Latin American Journal of Solids and Structures, 2017. **14**(12): p.2265-2290.
8. Vaghefpour, H., and Arvin, H., *Nonlinear free vibration analysis of pre-actuated isotropic piezoelectric cantilever nano-beams*. Microsystem Technologies, 2019. **25**: p.4097-4110.
9. Kaddar, M., Kaci, A., Bousahla, A. A., Tounsi, A., Bourada, F., Tounsi, A., Beida, E. A. A., Al-Osta, M. A., *A study on the structural behaviour of functionally graded porous plates on elastic foundation using a new quasi-3D model: Bending and free vibration analysis*. Computers and Concrete, 2020. **25**(1): p. 37-57.
10. Malekzadeh, K., and Sayyidmousavi, A., *Free vibration analysis of sandwich plates with a uniformly distributed attached mass, flexible core and different boundary conditions*. Journal of Sandwich Structures and Materials, 2010. **12**(6): p.709-732.
11. Demirtas, S., and Ozturk, H., *Effective mode shapes of multi-storey frames subjected to moving train loads*. Coupled Systems Mechanics, 2020. **9**(4): p.311-323.
12. Vinyas, M., *A higher-order free vibration analysis of carbon nanotube-reinforced magneto-electro-elastic plates using finite element methods.*Composites Part B: Engineering, 2021. **158**: p.286-301.
13. Safarpour, M., Rahimi, A. R., and Alibeigloo, A., *Static and free vibration analysis of graphene platelets reinforced composite truncated conical shell, cylindricall shell, and annular plate using theory of elasticity and DQM*. Mechanics Based Design of Structures and Machines, 2020. **48**(4): p.496-524.
14. Rahimi, A., Alibeigloo, A., and Safarpour M., *Three-dimensional static and free vibration analysis of graphene platelet reinforced porous composite cylindrical shell*. Journal of Vibration and Control, 2020. **26**(19-20): p.1627-1645.
15. Sahla, M., Saidi, H., Draiche, K., Bousahla, A. A., Bourada, F., Tounsi, A., *Free vibration analysis of angle-ply laminated composite and soft core sandwich plates.* Steel and Composite Structures, 2019. **33**(5): p.663-679.
16. Yan, Y., Liu, B., Xing, Y., Carrera, E., and Pagani, A., *Free vibration analysis of variable stiffness composite laminated beams and plates by novel hierarchical differential quadrature finite elements*. Composite Structures, 2021. **274**; 114364.
17. Bidgoli, E. M. R., and Arefi, M., *Free vibration analysis of micro plate reinforced with functionally graded nanoplatelets based on modified strain-gradient formulation*. Journal of Sandwich Structures and Materials, 2021. **23**(2), p.436-472.
18. Kıral, Z., *Harmonic response analysis of symmetric laminated composite beams with different boundary conditions*. Science and Engineering of Composite Materials, 2014. **21**(4): p.559-569.
19. Ramesha, C. M., Abhijith, K. G., Singh, A., Raj, A., and Naik, C. S., *Modal analysis and harmonic response analysis of a crankshaft*. International Journal of Emerging Technology and Advanced Engineering, 2015. **5**(6): 323-327.
20. Yu, Y., Zhang, S., Li, H., Wang, X., and Tiang, Y., *Modal and harmonic response analysis of key components of ditch device based on ANSYS*. Procedia Engineering, 2017. **174**: p.956-964.
21. Zhang, C., Jin, G., Ye, T., and Zhang, Y., *Harmonic response analysis of coupled plate structures using the dynamic stiffness method*. Thin-Walled Structures, 2018. **127**: p.402-415.
22. Jiaqiang, E., Liu, G., Liu, T., Zhang, Z., Zuo, H., Hu, W., and Wei, K., *Harmonic response analysis of a large dish solar thermal power generation system with wind-induced vibration*. Solar Energy, 2019. **181**: p.116-129.
23. Çeçen, F., and Aktaş, B., *Modal and harmonic response analysis of new CFRP laminate reinforced concrete railway sleepers.* Engineering Failure Analysis, 2021. **127**: 105471.
24. Rahmani, M., and Moslemi Petrudi, A., *Nonlinear vibration and dynamic response of nano composite conical tube by conveying fluid flow*. International Advanced Researches

and Engineering Journal, 2020. **4**(3): p.180-190.

25. Cruceanu, I. C., and Sorohan, S., *Determination of the harmonic response of a railway wheelset using the finite element analysis method*. Procedia Manufacturing, 2020. **46**: p.173-179.
26. Zeng, J., Chen, K., Ma, H., Duan, T., and Wen, B., *Vibration response analysis of a cracked rotating compressor blade during run-up process*. Mechanical Systems and Signal Processing, 2019. **118**: p.568-583.
27. Jena, R. M., Chakravety, S., and Jena, S. K., *Dynamic response analysis of fractionally damped beams subjected to external loads using homotopy analysis method*. Journal of Applied and Computational Mechanics, 2019. **5**(2); p.355-366.
28. Gawryluk, J., Mitura, A., and Teter, A., *Dynamic response of a composite beam rotating at constant speed caused by harmonic excitation with MFC actuator*. Composite Structures, 2019. **210**; p. 657-662.
29. Son, L., Surya, M., Bur, M., Ubaidillah, U., and Dhelika, R., *Shock and harmonic response analysis of UAV nose landing gear system with air damper*. Cogent Engineering, 2021. **8**(1): 1905231.
30. Kumar, M., and Sarangi, S. K., *Harmonic response of carbon nanotube reinforced functionally graded beam by finite element method*. Materials Today: Proceedings, 2021. **44**(6): p.4531-4536.
31. Praharaj, R. K., and Datta, N., *Dynamic response of plates resting on a fractional viscoelastic foundation and subjected to a moving load*. Mechanics Based Design of Structures and Machines, 2020. p. 1-16.
32. Abed, Z: A. K., and Majeed, W. I., *Effect of boundary conditions on harmonic response of laminated plates*. Composite Materials and Engineering, 2020. **2**(2): p.125-140.
33. Aghazadeh, R., *Dynamics of axially functionally graded pipes conveying fluid using a higher order shear deformation theory*. International Advanced Researches and Engineering Journal, 2021. **5**(2): p.209-217.
34. Liu, J., Fei, Q., Wu, S., Zhang, D., and Jiang, D., *Dynamic response of curvilinearly stiffened plates under thermal environment*. Journal of Mechanical Science and Technology, 2021. **35**: p.2359-2367.
35. Alavi, S. H., and Eipakchi, H., *An analytical approach for dynamic response of viscoelastic annular sector plates*. Mechanics of Advanced Materials and Structures, 2021. p. 1-17.
36. Heydarpour, Y., Mohammadzaheri, M., Ghodsi, M., Soltani, P., Al-Jahwari, F., Bahadur, I., and Al-Amri, B., *A coupled DQ-Heaviside-NURBS approach to investigate nonlinear dynamic response of GRE cylindrical shells under impulse loads*. Thin-Walled Structures, 2021,**165**: 107958.
37. Yulin, F., Lizhong, J., and Zhou, W., *Dynamic response of a three-beam system with intermediate elastic connections under a moving load/mass-spring.* Earthquake Engineering and Vibration, 2020, **19**(2): p.377-395.
38. Eyvazian, A., Shahsavari, D., and Karami, B., *On the dynamic of graphene reinforced nanocomposite cylindrical shells subjected to a moving harmonic load.* International Journal of Engineering Science, **154**: 103339.
39. Oke, W. A., and Khulief, Y. A., *Dynamic response analysis of composite pipes conveying fluid in the presence of internal wall thinnhing.* Journal of Engineering Mechanics, 2020, **146**(10): 04020118.
40. Ansys® Training Manual [cited 2021 21 July], Available from: http://www.eng.lbl.gov/~als/FEA/ANSYS_V9_INFO/Workbench_Simulation_9.0_Intro_3rd_Edition/ppt/AWS90_Ch10_Harmonic.ppt.
41. Petyt, M., *Introduction to Finite Element Vibration Analysis*. 2010, USA: New York.
42. Ansys® Workbench, Release 18.2, Harmonic Response Analysis.